Q^2 evolution of chiral-odd twist-3 distribution $e(x, Q^2)$

Yuji Koike and N. Nishiyama

Graduate School of Science and Technology, Niigata University, Ikarashi, Niigata 950-21, Japan

Abstract

We study the Q^2 dependence of the chiral-odd twist-3 distribution $e(x, Q^2)$. The anomalous dimension matrix for the corresponding twist-3 operators is calculated in the one-loop level. This study completes the calculation of the anomalous dimension matrices for all the twist-3 distributions together with the known results for the other twist-3 distributions $g_2(x, Q^2)$ and $h_L(x, Q^2)$. We also have confirmed that in the large N_c limit the Q^2-evolution of $e(x, Q^2)$ is wholely governed by the lowest eigenvalue of the anomalous dimension matrix which takes a very simple analytic form as in the case of g_2 and h_L.

PACS numbers: 12.38.Bx; 11.10.Hi; 11.15.Pg; 13.85.Qk

1 Introduction

Ongoing plans of high energy collider experiments are going on their way toward more precision measurements and more variety of spin-dependent observables in many (semi) inclusive processes. Correspondingly, increasing attention is paid on the power corrections due to the higher twist-effects which represent parton correlations in the target. Recent measurement of the nucleon's g_2 structure function by the E143 collaboration [1] anticipates a forthcoming significant progress of the twist-3 physics. Under this circumstance, QCD study on the scale dependence of various distribution and fragmentation functions is of great interest.

The nucleon has three twist-3 distributions g_2, h_L and e [2]. g_2 is chiral-even and the other two are chiral-odd. e is spin-independent and the other two are spin-dependent. Compared to $e(x, Q^2)$, g_2 and h_L have more chance to be measured experimentally since they become leading contribution to proper asymmetries in the polarized deep inelastic scattering (DIS) and Drell-Yan processes, respectively. Their Q^2 evolution has been studied in [3, 4, 5] for g_2 and in [6, 7] for h_L.

Similarly to the distribution functions, there are three twist-3 fragmentation functions which describes hadronization processes of partons in semi-inclusive processes [8], $\hat{g}_2(z, Q^2)$, $\hat{h}_L(z, Q^2)$ and $\hat{e}(z, Q^2)$. (Their naming is parallel to the corresponding distribution functions.) In the inclusive pion production in the transversely polarized DIS, the chiral-odd fragmentation function $\hat{e}$ of the pion appears as a leading contribution together with h_1 (twist-2) of the nucleon. Although the Q^2 evolution of the twist-2 fragmentation functions is known to be obtained from that of the corresponding distributions in the one-loop level (Gribov-Lipatov reciprocity [9]), no such relation is known for the higher twist fragmentation functions.

In this paper we investigate the Q^2 evolution of $e(x, Q^2)$. Theoretically, this completes the calculation of the anomalous dimension matrices of all the twist-3 distributions. Phenomenologically, we expect it will shed light on the Q^2 evolution of $\hat{e}(z, Q^2)$, anticipating the day when their relation is clarified.

The outline of this paper is the following: In section 2, we briefly recall the twist-3

operators for $e(x,Q^2)$ [2]. Similarity to the h_L case is reminded. In section 3, we present the calculation of the one-loop anomalous dimension matrix for $e(x,Q^2)$. The method follows that of [6]. In section 4, the Q^2 evolution of $e(x,Q^2)$ in the large N_c limit is discussed. This part is a recapitulation of [7] in our language. Section 5 is devoted to a brief summary of our results. Appendix contains the contributions from each one-loop Feynman diagram.

2 Twist-3 operators for $e(x,Q^2)$

The chiral-odd twist-3 distribution function $e(x,Q^2)$ is defined by the relation [2]

$$\int \frac{d\lambda}{2\pi} e^{i\lambda x} \langle P|\bar{\psi}(0)\psi(\lambda n)|_Q|P\rangle = 2Me(x,Q^2), \tag{2.1}$$

where $|P\rangle$ is the nucleon (mass M) state with momentum P. Two light-like vectors p and n defined by the relation, $P = p + \frac{M^2}{2}n$, $p^2 = n^2 = 0$, $p\cdot n = 1$, specify the Lorentz frame of the system. Gauge-link operators are implicit in (2.1). Taking the moments of (2.1) with respect to x, one can express the moments of $e(x,Q^2)$ in terms of the nucleon matrix elements of the twist-3 operators $V^{\mu_1\cdots\mu_n}$:

$$\begin{aligned}
\mathcal{M}_n\left[e(Q^2)\right] &= e_n(Q^2), &(2.2)\\
\langle PS|V^{\mu_1\mu_2\cdots\mu_n}|PS\rangle &= 2e_n M(P^{\mu_1}P^{\mu_2}\cdots P^{\mu_n} - \text{traces}), &(2.3)\\
V^{\mu_1\mu_2\cdots\mu_n} &= \mathcal{S}_n\bar{\psi}iD^{\mu_1}iD^{\mu_2}\cdots iD^{\mu_n}\psi - \text{traces}, &(2.4)
\end{aligned}$$

where $\mathcal{M}_n\left[e(Q^2)\right] \equiv \int_{-1}^{1} dx\, x^n e(x,Q^2)$ and the covariant derivative $D_\mu = \partial_\mu - igA_\mu$ restores the gauge invariance. As in (2.3) and (2.4), we often suppress the explicit scale dependence. Following a common wisdom we introduce a null vector Δ_μ ($\Delta^2 = 0$) to kill the trace terms of $V^{\mu_1\cdots\mu_n}$ and introduce the notation $V_n\cdot\Delta \equiv V^{\mu_1\cdots\mu_n}\Delta_{\mu_1}\cdots\Delta_{\mu_n}$ for convenience, and similarly for other operators in the following. Using the relation $D^\mu = \frac{1}{2}\{\not{D},\gamma^\mu\}$ and $[D_\mu, D_\nu] = -igG_{\mu\nu}$ with the gluon field strength $G_{\mu\nu}$, $V_n\cdot\Delta$ can be recast into the following form:

$$V_n\cdot\Delta = \sum_{l=2}^{n} U_{n,l}\cdot\Delta + N_n\cdot\Delta + E_n\cdot\Delta, \tag{2.5}$$

where

$$U_l^{\mu_1\cdots\mu_n} = \frac{1}{2}\mathcal{S}_n\bar{\psi}\sigma^{\alpha\mu_1}iD^{\mu_2}\cdots gG^{\mu_l}{}_{\alpha}\cdots iD^{\mu_n}\psi - \text{traces}, \tag{2.6}$$

$$N^{\mu_1\cdots\mu_n} = \mathcal{S}_n m_q \bar{\psi}\gamma^{\mu_1} iD^{\mu_2}\cdots iD^{\mu_n}\psi - \text{traces}, \tag{2.7}$$

$$E^{\mu_1\cdots\mu_n} = \frac{1}{2}\mathcal{S}_n\left[\bar{\psi}(i\not{D} - m_q)\gamma^{\mu_1} iD^{\mu_2}\cdots iD^{\mu_n}\psi + \bar{\psi}\gamma^{\mu_1} iD^{\mu_2}\cdots iD^{\mu_n}(i\not{D} - m_q)\psi\right] - \text{traces}. \tag{2.8}$$

U_l contains $G_{\mu\nu}$ explicitly, which indicates that $e(x)$ represents the quark-gluon correlations in the nucleon. N is the quark mass times the twist-2 operator which contributes to the moments of f_1 structure function familiar in the spin-averaged DIS. E is the EOM (equation of motion) operator which vanishes by use of the QCD equation-of-motion. Although the physical matrix elements of EOM operators vanish, one needs to take into account the mixing with E to carry out the renormalization of U and N, as is discussed in [5, 6] in the context of the renormalization of g_2 and h_L. From (2.5) one sees that U_l appears in the form of

$$R_{n,l}^{\mu_1\cdots\mu_n} = U_{n-l+2}^{\mu_1\cdots\mu_n} + U_l^{\mu_1\cdots\mu_n}, \quad \left(l = 2, ..., \left[\frac{n}{2}\right] + 1\right). \tag{2.9}$$

By this combination, $R_{n,l}$ has a definite charge conjugation $(-1)^n$. Readers may recall the similarity between the present $\{U_l,\, R_{n,l}\}$ and $\{\theta_l,\, R_{n,l}\}$ which appeared in h_L [2, 6]. In fact presence of γ_5 in θ_l is the mere difference from U_l. $R_{n,l}$ of h_L is defined as $\theta_{n-l+2} - \theta_l$ and has a charge conjugation $(-1)^{n+1}$ which is opposite to the above $R_{n,l}$ in (2.9). We will see the similarity in the renormalization constants between h_L and e in the following.

3 Q^2 evolution of $e(x, Q^2)$

For the renormalization of $e(x)$, we closely follow the method of [6] which discussed the renormalization of h_L. So we omit the detail in the following. Owing to the chiral-odd nature, $e(x)$ does not mix with the gluon-distribution. We choose $R_{n,l}$ $(l = 2, \ldots, \left[\frac{n}{2}\right] + 1)$, E, N as a basis of the operators. For the renormalization of $R_{n,l}$, we calculate the one-loop correction to the three-point function $F_\mu(p, q, p - q)$ defined by

$$\begin{aligned} &F_\mu(p, q, k)(2\pi)^4\delta^4(p + k - q)G(p)G(q)D(k) \\ &\quad = \int d^4x d^4y d^4z e^{ipx} e^{-iqy} e^{ikz}\langle T\{\mathcal{O}\psi(x)\bar{\psi}(y)A_\mu(z)\}\rangle, \quad (\mathcal{O} = R_{n,l},\ N,\ E) \end{aligned} \tag{3.1}$$

where G and D are, respectively, the quark and gluon propagators. (We suppressed the Lorentz and spinor indices for simplicity.) In order to take into account the mixing with the

EOM operator properly, we use off-shell kinematics for the external lines. The calculation is done with the Feynman gauge for the gluon propagator (of course the result should be independent of the gauge) and the MS scheme is adopted with the dimensional regularization. The three-point basic vertices shown in Fig. 1(a) for $R_{n,l}\cdot\Delta$, $E_n\cdot\Delta$, $N_n\cdot\Delta$ are calculated to be

$$\mathcal{R}^{(3)}_{n,l,\mu} = -i\frac{g}{2}\sigma^{\alpha\lambda}\Delta_\lambda(\hat{p}^{n-l}\hat{q}^{l-2}+\hat{p}^{l-2}\hat{q}^{n-l})(-\hat{k}g_{\alpha\mu}+k_\alpha\Delta_\mu)t^a, \tag{3.2}$$

$$\mathcal{E}^{(3)}_{n,\mu} = \frac{g}{2}\Bigg[\gamma_\mu\not{\Delta}\hat{q}^{n-1}+\not{\Delta}\hat{p}^{n-1}\gamma_\mu+\Delta_\mu\sum_{j=2}^{n}(\not{p}-m_q)\not{\Delta}\hat{p}^{j-2}\hat{q}^{n-j} + \Delta_\mu\sum_{j=2}^{n}\not{\Delta}(\not{q}-m_q)\hat{p}^{j-2}\hat{q}^{n-j}\Bigg]t^a, \tag{3.3}$$

$$\mathcal{N}^{(3)}_{n,\mu} = m_q g\Delta_\mu\not{\Delta}\sum_{j=2}^{n}\hat{p}^{j-2}\hat{q}^{n-j}t^a, \tag{3.4}$$

where $k=q-p$, $\hat{p}=p\cdot\Delta$ for an arbitrary four vector p and t^a is the color matrix normalized as $\mathrm{Tr}(t^at^b)=\frac{1}{2}\delta^{ab}$. One-loop diagrams for the above F_μ are shown in Fig. 2. In calculating these diagrams, we need a Feynman rule for the four-point basic vertex of $R_{n,l}\cdot\Delta$ shown in Fig. 1(b). It is given by

$$\begin{aligned}&\frac{g^2}{2}\Big[f^{abc}t^c\sigma^{\alpha\lambda}\Delta_\lambda\Delta_\mu g_{\alpha\nu}\hat{p}^{n-l}\hat{q}^{l-2}\\ &-i\sigma^{\alpha\lambda}\Delta_\lambda t^at^b\sum_{j=2}^{n-l+1}\hat{p}^{j-2}\Delta_\mu(\hat{p}+\hat{k})^{n-l+1-j}(-\hat{k}'g_{\alpha\nu}+k'_\alpha\Delta_\nu)\hat{q}^{l-2}\\ &-i\sigma^{\alpha\lambda}\Delta_\lambda t^at^b\sum_{j=n-l+3}^{n}\hat{p}^{n-l}\Delta_\nu(\hat{p}+\hat{k})^{j-n+l-3}(-\hat{k}g_{\alpha\mu}+k_\alpha\Delta_\mu)\hat{q}^{n-j}\\ &+(\mu\leftrightarrow\nu,k\leftrightarrow k',a\leftrightarrow b)\Big]+(l\to n-l+2).\end{aligned} \tag{3.5}$$

For the actual calculation of the one-loop diagrams, we introduce a vector Ω_μ with the condition $\Omega\cdot\Delta=0$, and consider $F_\mu\Omega^\mu$ [6]. This way mixing with the gauge noninvariant EOM operators can be avoided and the calculation is greatly simplified. (See [6] for the detail.) The contraction of $\mathcal{R}^{(3)}_{n,l,\mu}$ and $\mathcal{E}^{(3)}_{n,l,\mu}$ with Ω_μ leads to

$$\mathcal{R}^{(3)}_{n,l}\cdot\Omega = \frac{ig}{2}\Omega_\alpha\sigma^{\alpha\lambda}\Delta_\lambda(\hat{q}-\hat{p})\left(\hat{p}^{n-l}\hat{q}^{l-2}+\hat{p}^{l-2}\hat{q}^{n-l}\right)t^a, \tag{3.6}$$

$$\mathcal{E}^{(3)}_{n}\cdot\Omega = -\frac{ig}{2}\Omega_\alpha\sigma^{\alpha\lambda}\Delta_\lambda\left(\hat{q}^{n-1}-\hat{p}^{n-1}\right)t^a. \tag{3.7}$$

The mixing coefficients between $R_{n,l}$ and $\{N,\, E\}$, Z_{lE} and Z_{lN}, can also be obtained from the one-loop correction to the two point function shown in Fig. 3 (b), (c), giving a consistency check. The two point basic vertices for E and N are

$$\mathcal{E}_n^{(2)} = \frac{1}{2}\hat{p}^{n-1}\left(\not{\Delta}\not{p} + \not{p}\not{\Delta} - 2m_q\not{\Delta}\right), \tag{3.8}$$

$$\mathcal{N}_n^{(2)} = m_q\hat{p}^{n-1}\not{\Delta}. \tag{3.9}$$

Using these Feynman rules for the vertices, one can calculate the one-loop diagrams shown in Figs. 2 and 3. Actual calculation is very tedious and will be described in the Appendix in detail. Taking into account the wave function renormalization for the fields and the renormalization for m_q and g which explicitly appear in the vertices [6], we eventually obtained the renormalization constants Z_{ij} among $R_{n,l}$, N and E in the following matrix form:

$$\begin{pmatrix} R_{n,l}^B \\ E_n^B \\ N_n^B \end{pmatrix} = \begin{pmatrix} Z_{lm}(\mu) & Z_{lE}(\mu) & Z_{lN}(\mu) \\ 0 & Z_{EE}(\mu) & 0 \\ 0 & 0 & Z_{NN}(\mu) \end{pmatrix} \begin{pmatrix} R_{n,m}(\mu) \\ E_n(\mu) \\ N_n(\mu) \end{pmatrix}, \quad \left(l, m = 2, \cdots, \left[\frac{n}{2}\right] + 1\right). \tag{3.10}$$

Z_{ij} can be expressed as

$$Z_{ij} = \delta_{ij} + \frac{g^2}{16\pi^2\varepsilon}Y_{ij} \qquad \left(i, j = 2, \cdots, \left[\frac{n}{2}\right] + 1, E, N\right) \tag{3.11}$$

with $\varepsilon = \frac{4-d}{2}$ (d is the space-time dimension in the dimensional regularization) and the constants Y_{ij} given below. To write down Y_{ij} we define a symbol $\langle\frac{n}{2}\rangle$ as $\langle\frac{n}{2}\rangle \equiv [\frac{n}{2}] = \frac{n}{2}$ for an even n and $\langle\frac{n}{2}\rangle \equiv [\frac{n}{2}] + 1 = \frac{n+1}{2}$ for an odd n. Then Y_{ij} is given as follows:

$$\begin{aligned} Y_{lm} &= C_G\left[\frac{(m-1)(m+l)}{2(l-m)[l-1]_2} + \frac{(m-1)(m+n-l+2)}{2(n-l-m+2)[n-l+1]_2} - \frac{1}{l} - \frac{1}{n-l+2}\right. \\ &\quad \left. + \frac{(l-3)(l+1-m)}{2[l-1]_3} + \frac{l+2}{2[l-1]_2} + \frac{(n-l-1)(n-l-m+3)}{2[n-l+1]_3} + \frac{n-l+4}{2[n-l+1]_2}\right] \\ &\quad + (2C_F - C_G)\left[\frac{(-1)^{n-l-m}\ {}_{n-l}C_{m-2}}{(n-l+2-m)\ {}_{n-m+1}C_{l-1}} + \frac{(-1)^{l-m}\ {}_{l-2}C_{l-m}}{(l-m)\ {}_{n-m+1}C_{l-m}}\right. \\ &\quad \left. - 2(-1)^m\left(\frac{{}_{l-1}C_{m-1}}{[l-1]_3} + \frac{{}_{n-l+1}C_{m-1}}{[n-l+1]_3}\right)\right] \\ &\quad (2 \le l \le \left[\frac{n}{2}\right] + 1, \quad 2 \le m \le l-1), \end{aligned} \tag{3.12}$$

$$
\begin{aligned}
Y_{ll} &= C_G\left[-S_{l-1}-S_{n-l+1}-\frac{1}{2l}-\frac{1}{2(n-l+2)}+\frac{(l-1)(n+2)}{2(n-2l+2)[n-l+1]_2}\right.\\
&\quad -\frac{2}{n-l+2}-\frac{1}{l}\\
&\quad \left.+\frac{l-3}{2[l-1]_3}+\frac{l+2}{2[l-1]_2}+\frac{(n-l-1)(n-2l+4)}{2[n-l+1]_3}+\frac{n-l+4}{[n-l+1]_2}\right]\\
&\quad +2(C_G-2C_F)\left[(-1)^l\left(\frac{1}{[l-1]_3}+\frac{(-1)^n+\ {}_{n-l+1}C_{l-1}}{[n-l+1]_3}\right)\right.\\
&\quad \left.-(-1)^n\frac{l-1}{2(n-l+1)(n-2l+2)}\right]\\
&\quad -C_F\left(2S_{l-1}+2S_{n-l+1}-3\right)\qquad \left(2\le l\le\left\langle\frac{n}{2}\right\rangle\right), \qquad (3.13)
\end{aligned}
$$

$$
\begin{aligned}
Y_{\frac{n}{2}+1\ \frac{n}{2}+1} &= C_G\left[-2S_{\frac{n}{2}}-\frac{6}{n+2}+\frac{\frac{n}{2}-2}{\left[\frac{n}{2}\right]_3}+\frac{\frac{n}{2}+3}{\left[\frac{n}{2}\right]_2}\right]+(2C_F-C_G)4\frac{(-1)^{\frac{n}{2}}}{\left[\frac{n}{2}\right]_3}\\
&\quad +C_F\left(3-4S_{\frac{n}{2}}\right)\qquad\qquad (\text{for even } n), \qquad (3.14)
\end{aligned}
$$

$$
\begin{aligned}
Y_{lm} &= C_G\left[\frac{(2n-l-m+4)(n-m+1)}{2(m-l)[n-l+1]_2}+\frac{(m-1)(m+n-l+2)}{2(n-m-l+2)[n-l+1]_2}\right.\\
&\quad \left.-\frac{2}{n-l+2}+\frac{(n-l-1)(n-2l+4)}{2[n-l+1]_3}+\frac{n-l+4}{[n-l+1]_2}\right]\\
&\quad +(C_G-2C_F)\left[\frac{2(-1)^m\left\{{}_{n-l+1}C_{m-1}+(-1)^n\ {}_{n-l+1}C_{m-l}\right\}}{[n-l+1]_3}\right.\\
&\quad \left.-(-1)^{m-l}\left(\frac{{}_{n-l}C_{m-l}}{(m-l)\ {}_{m-1}C_{m-l}}+\frac{(-1)^n\ {}_{n-l}C_{m-2}}{(n-l+2-m)\ {}_{n-m+1}C_{l-1}}\right)\right]\\
&\quad \left(3\le l+1\le m\le\left\langle\frac{n}{2}\right\rangle\right), \qquad (3.15)
\end{aligned}
$$

$$
\begin{aligned}
Y_{l\ \frac{n}{2}+1} &= C_G\left[\frac{1}{4}\frac{1}{[n-l+1]_2}\frac{n(3n-2l+6)}{n-2l+2}-\frac{1}{n-l+2}\right.\\
&\quad \left.+\frac{1}{2}\left(\frac{(n-l-1)(\frac{n}{2}-l+2)}{[n-l+1]_3}+\frac{n-l+4}{[n-l+1]_2}\right)\right]\\
&\quad +(2C_F-C_G)\left(\frac{2(-1)^{\frac{n}{2}}}{[n-l+1]_3}\ {}_{n-l+1}C_{\frac{n}{2}}+\frac{(-1)^{\frac{n}{2}-l+1}}{\frac{n}{2}-l+1}\frac{{}_{n-l}C_{\frac{n}{2}-l+1}}{{}_{\frac{n}{2}}C_{l-1}}\right)
\end{aligned}
$$

$$\left(\text{for even } n, \quad 2 \le l \le \frac{n}{2}\right), \tag{3.16}$$

$$Y_{lE} = -2C_F \left(\frac{1}{[l]_2} + \frac{1}{[n-l+2]_2}\right) \qquad \left(2 \le l \le \left[\frac{n}{2}\right] + 1\right), \tag{3.17}$$

$$Y_{lN} = 4C_F \left(\frac{1}{[l-1]_3} + \frac{1}{[n-l+1]_3}\right) \qquad \left(2 \le l \le \left[\frac{n}{2}\right] + 1\right), \tag{3.18}$$

$$Y_{EE} = 2(1 - S_n)C_F, \tag{3.19}$$

$$Y_{NN} = C_F \left(\frac{2}{n(n+1)} - 4S_n\right), \tag{3.20}$$

where $C_F = \frac{N_c^2-1}{2N_c}$ and $C_G = N_c$ are the Casimir operators of the gauge group $SU(N_c)$, $S_n = \sum_{j=1}^{n} 1/j$, $[j]_k = j(j+1)\cdots(j+k-1)$, and ${}_nC_l$ is the binomial coefficient defined as ${}_nC_l = n!/l!(n-l)!$. Note that (3.16) is one half of (3.15) with $m = \frac{n}{2} + 1$ for even n. With these Y_{ij} $(i, j = 2, 3, ..., \left[\frac{n}{2}\right] + 1,\ E,\ N)$, the anomalous dimension matrix for the twist-3 operators $R_{n,l}$, E and N take the form of the upper triangular matrix as

$$\gamma_{ij} = -\frac{g^2}{8\pi^2} Y_{ij}. \tag{3.21}$$

The above results for Y can be compared with the mixing matrix X for h_L given in Eqs. (3.14)-(3.20) of [6]. Their difference comes from the opposite charge conjugation symmetry of $R_{n,l}$. Solving the renormalization group equation, the Q^2 evolution of $R_{n,l}$ and N is given by

$$a_{n,l}(Q^2) = \sum_{m=2}^{[\frac{n}{2}]+1} \left[\left(\frac{\alpha(Q^2)}{\alpha(\mu^2)}\right)^{-Y/b_0}\right]_{lm} a_{n,m}(\mu^2) + \left[\left(\frac{\alpha(Q^2)}{\alpha(\mu^2)}\right)^{-Y/b_0}\right]_{lN} d_n(\mu^2), \tag{3.22}$$

$$d_n(Q^2) = \left(\frac{\alpha(Q^2)}{\alpha(\mu^2)}\right)^{-Y_{NN}/b_0} d_n(\mu^2), \tag{3.23}$$

where $a_{n,l}$ and d_n are defined by

$$\langle P|R_{n,l}^{\mu_1\cdots\mu_n}(\mu^2)|P\rangle = 2a_{n,l}(\mu^2) M\mathcal{S}_n(P^{\mu_1}\cdots P^{\mu_n} - \text{traces}), \tag{3.24}$$

$$\langle P|N^{\mu_1\cdots\mu_n}(\mu^2)|P\rangle = 2d_n(\mu^2) M\mathcal{S}_n(P^{\mu_1}\cdots P^{\mu_n} - \text{traces}), \tag{3.25}$$

and $b_0 = \frac{11}{3}N_c - \frac{2}{3}N_f$.

The complete spectrum of the eigenvalues of the anomalous dimension matrix (3.21) (ignoring the factor $g^2/8\pi^2$) is shown in Fig. 4(a) together with those for the twist-2 distribution h_1. One sees from the figure that the anomalous dimensions of e are significantly larger than those of h_1, except for the first several moments.

Before closing this section, we compare the Q^2 evolution among the twist-2 and -3 distributions (at $m_q = 0$), using the first few moments. For $n = 2$ and 3, only one operator contributes to $e(x)$. The values of Y can be read from (3.13) and (3.14) as $Y^{n=2} = \frac{-55}{9}$ and $Y^{n=3} = \frac{-73}{9}$. Thus the Q^2 evolution becomes

$$\mathcal{M}_2\left[e(Q^2)\right] = L^{6.11/b_0}\mathcal{M}_2\left[e(\mu^2)\right], \qquad \mathcal{M}_3\left[e(Q^2)\right] = L^{8.11/b_0}\mathcal{M}_3\left[e(\mu^2)\right], \tag{3.26}$$

where $L = \frac{\alpha(Q^2)}{\alpha(\mu^2)}$. In table 1, we summarize the anomalous dimensions of the twist-2 and -3 distributions for $n = 2$, 3, ignoring the common factor $g^2/8\pi^2$. One sees that these moments of e evolve slower than those of the other twist-3 distributions and are close to the twist-2 distributions.

n	f_1, g_1	h_1	e	$\tilde{g}_2$	$\tilde{h}_L$
2	$\frac{50}{9}$	$\frac{52}{9}$	$\frac{55}{9}$	$\frac{77}{9}$	–
3	$\frac{314}{45}$	$\frac{64}{9}$	$\frac{73}{9}$	–	$\frac{104}{9}$

Table 1. The anomalous dimensions for the 2nd and 3rd moments of the nonsinglet twist-2 and twist-3 distributions. For these moments, the twist-3 distributions receive the contribution from only one operator. $\tilde{h}_L$ and $\tilde{g}_2$ denote the twist-3 parts of h_L and g_2, respectively. For $\tilde{h}_L$, the third moment is the lowest one, and the result is taken from [6]. For g_2, the result is taken from [3], and the anomalous dimensions for odd moments are not available because they have been discussed in the context of DIS.

4 Large N_c limit

In [4, 7], it has been proved that all the (nonsinglet) twist-3 distributions g_2, h_L and e obey a simple GLAP equation [10] similarly to the twist-2 distributions in the $N_c \to \infty$ limit. In this limit, Q^2 evolution of these distributions is completely determined by the lowest eigenvalue of the anomalous dimension matrix which has a simple analytic form. For e, this can be

checked using the results in the previous section. At $N_c \to \infty$, i.e., $C_F \to N_c/2$, the lowest eigenvalue of γ in (3.21) is given by (ignoring the factor $g^2/8\pi^2$)

$$\gamma_n^e = 2N_c \left(S_n - \frac{1}{4} - \frac{1}{2(n+1)} \right). \tag{4.1}$$

As was shown in section 2, the n-th moment of $e(x)$ can be expressed in terms of $a_{n,l}$ as

$$\mathcal{M}_n[e] = \sum_{l=2}^{\langle \frac{n}{2} \rangle} a_{n,l} \left\{ +\frac{1}{2} a_{n,[\frac{n}{2}]+1} \quad n: \text{ even} \right\}, \tag{4.2}$$

where $\{\cdots \ n: \text{ even}\}$ means this term is only for even n. We can directly check that the coefficients of $a_{n,l}$ in (4.2) constitute the *left* eigenvector of the mixing matrix Y with the eigenvalue $-\gamma_n^e$, i.e.,

$$\sum_{l=2}^{[\frac{n}{2}]+1} Y_{lm} = -\gamma_n^e \qquad \left(m = 2, \cdots, \left[\frac{n}{2} \right] + 1 \right) \tag{4.3}$$

for odd n and

$$\begin{aligned} &\sum_{l=2}^{[\frac{n}{2}]} Y_{lm} + \frac{1}{2} Y_{\frac{n}{2}+1\ m} = -\gamma_n^e \qquad \left(m = 2, \cdots, \left[\frac{n}{2} \right] \right), \\ &\sum_{l=2}^{[\frac{n}{2}]} Y_{l\ \frac{n}{2}+1} + \frac{1}{2} Y_{\frac{n}{2}+1\ \frac{n}{2}+1} = -\frac{1}{2} \gamma_n^e \end{aligned} \tag{4.4}$$

for even n. This means all the *right* eigenvectors except the one which corresponds to γ_n^e are orthogonal to the above vector consisting of the coefficients of $a_{n,l}$ in (4.2). This proves that the Q^2 evolution of e is exactly given by

$$\mathcal{M}_n \left[e(Q^2) \right] = L^{\gamma_n^e/b_0} \mathcal{M}_n \left[e(\mu^2) \right], \tag{4.5}$$

as is found in [7] by a different method. The complete spectrum of the eigenvalues of the anomalous dimension matrix at large N_c is given in Fig. 4(b) together with the analytic result in (4.1). One sees that (4.1) indeed corresponds to the lowest eigenvalue.

To see how the approximation by the $N_c \to \infty$ result works, we compare the two results for $n = 4$, as an example. The exact mixing matrix is

$$Y = \begin{pmatrix} -\frac{511}{45} & \frac{21}{10} \\ \frac{10}{3} & -\frac{122}{9} \end{pmatrix}, \tag{4.6}$$

and the one at $N_c \to \infty$ is

$$Y = \begin{pmatrix} -\frac{119}{10} & \frac{9}{5} \\ 3 & -14 \end{pmatrix}. \tag{4.7}$$

From these Ys' one gets

$$\begin{aligned} \mathcal{M}_4\left[e(Q^2)\right] &= (0.983 a_{4,2}(\mu) + 0.520 a_{4,3}(\mu)) \left(\frac{\alpha(Q^2)}{\alpha(\mu^2)}\right)^{9.59/b_0} \\ &+ (0.017 a_{4,2}(\mu) - 0.020 a_{4,3}(\mu)) \left(\frac{\alpha(Q^2)}{\alpha(\mu^2)}\right)^{15.3/b_0} \end{aligned} \tag{4.8}$$

for the exact Q^2 evolution and

$$\mathcal{M}_4\left[e(Q^2)\right] = \left(a_{4,2}(\mu) + \frac{1}{2} a_{4,3}(\mu)\right) \left(\frac{\alpha(Q^2)}{\alpha(\mu^2)}\right)^{10.4/b_0} \tag{4.9}$$

at $N_c \to \infty$. Equations (4.8) and (4.9) can be compared with Eqs. (20) and (21) of [7] for h_L. One sees here again that the coefficients in the second term of (4.8) are small (i.e., $1/N_c^2$ suppressed) and the anomalous dimension in (4.9) is close to the smaller one in (4.8).

5 Summary

In this paper, we presented the covariant calculation of the anomalous dimension matrix for the chiral-odd twist-3 distribution $e(x, Q^2)$. The operator mixing with the EOM operator is taken into account. This study completes the whole list of the anomalous dimensions of all the twist-3 distributions in the one-loop level together with the known results for g_2 and h_L. At large N_c, we have confirmed that the lowest eigenvalues of the anomalous dimension matrix take a simple analytic form shown in (4.1) and it governs the whole Q^2 evolution of $e(x, Q^2)$ as was found in [7] by a different method.

Acknowledgement

We thank V.M. Braun and K. Tanaka for useful discussions.

Appendix

In this appendix we present the contribution from each one-loop Feynman diagram shown in Figs. 2 and 3.

First we consider the three-point function $F_\mu \Omega^\mu$ with the insertion of $R_{n,l} \cdot \Delta$. We set $m_q = 0$ to get Z_{lm} and Z_{lE} $(l, m = 2, \ldots [n/2] + 1)$.

Fig.2(a) gives 0.

Fig.2(b) gives

$$\begin{aligned}
&\frac{g^2}{16\pi^2\varepsilon} C_G \left[\sum_{m=2}^{l-1} \left(\frac{(l+m)(m-1)}{2(l-m)[l-1]_2} + \frac{(n-l+2+m)(m-1)}{2(n-l+2-m)[n-l+1]_2} \right) \mathcal{R}^{(3)}_{n,m} \right. \\
&\quad + \left(1 - S_{l-1} - S_{n-l+1} - \frac{1}{2l} - \frac{1}{2(n-l+2)} + \frac{(n+2)(l-1)}{2(n-2l+2)[n-l+1]_2} \right) \mathcal{R}^{(3)}_{n,l} \\
&\quad + \sum_{m=l+1}^{\langle n/2 \rangle} \left(\frac{(2n-l-m+4)(n-m+1)}{2(m-l)[n-l+1]_2} + \frac{(n-l+2+m)(m-1)}{2(n-l+2-m)[n-l+1]_2} \right) \mathcal{R}^{(3)}_{n,m} \\
&\quad \left. \left\{ + \frac{1}{4} \frac{1}{[n-l+1]_2} \frac{n(3n-2l+6)}{n-2l+2} \mathcal{R}^{(3)}_{n,\frac{n}{2}+1} \quad n: \text{ even} \right\} \right] \qquad \left(2 \le l \le \left\langle \frac{n}{2} \right\rangle \right), \qquad \text{(A.1)}
\end{aligned}$$

where $\{\cdots \; n: \text{ even}\}$ means this term is only for an even n and its coefficient is one half of that of the third line with $m = [n/2] + 1$ (the same in (A.3), (A.5) and (A.7) below), and

$$\begin{aligned}
&\frac{g^2}{16\pi^2\varepsilon} C_G \left[\sum_{m=2}^{[\frac{n}{2}]} \left(\frac{2}{\frac{n}{2} - m + 1} - \frac{n+m+1}{\left[\frac{n}{2}\right]_2} \right) \mathcal{R}^{(3)}_{n,m} \right. \\
&\quad \left. + \left(1 - S_{\frac{n}{2}} - S_{\frac{n}{2}+1} \right) \mathcal{R}^{(3)}_{n,\frac{n}{2}+1} \right] \qquad \left(\text{for } l = [\frac{n}{2}] + 1 \text{ with even } n \right). \qquad \text{(A.2)}
\end{aligned}$$

In (A.2), the terms with $m = 2, \ldots, [n/2]$ are the same as the first line of (A.1) with $l = [n/2] + 1$. This rule also applies to the results for other diagrams.

Fig.2(c) + Fig.2(d) gives

$$\begin{aligned}
&\frac{g^2}{16\pi^2\varepsilon} (2C_F - C_G) \left[\sum_{m=2}^{l-1} 2(-1)^{m-1} \left(\frac{{}_{n-l+1}C_{m-1}}{[n-l+1]_3} + \frac{{}_{l-1}C_{m-1}}{[l-1]_3} \right) \mathcal{R}^{(3)}_{n,m} \right. \\
&\quad + 2(-1)^{l-1} \left(\frac{{}_{n-l+1}C_{l-1} + (-1)^n}{[n-l+1]_3} + \frac{1}{[l-1]_3} \right) \mathcal{R}^{(3)}_{n,l} \\
&\quad + \sum_{m=l+1}^{\langle n/2 \rangle} \frac{2(-1)^{m-1}}{[n-l+1]_3} \left({}_{n-l+1}C_{m-1} + (-1)^n \, {}_{n-l+1}C_{m-l} \right) \mathcal{R}^{(3)}_{n,m} \\
&\quad \left\{ + \frac{2(-1)^{\frac{n}{2}}}{[n-l+1]_3} \, {}_{n-l+1}C_{\frac{n}{2}} \mathcal{R}^{(3)}_{n,\frac{n}{2}+1} \quad n: \text{ even} \right\} \\
&\quad \left. - \left(\frac{1}{[l]_2} + \frac{1}{[n-l+2]_2} \right) \mathcal{E}^{(3)}_n \right] \qquad \left(2 \le l \le \left\langle \frac{n}{2} \right\rangle \right), \qquad \text{(A.3)}
\end{aligned}$$

and

$$\frac{g^2}{16\pi^2\varepsilon}(2C_F - C_G)\left[\sum_{m=2}^{[n/2]+1} 4(-1)^{m-1}\frac{{}_{\frac{n}{2}}C_{m-1}}{[n/2]_3}\mathcal{R}^{(3)}_{n,m} - \frac{2}{\left[\frac{n}{2}+1\right]_2}\mathcal{E}^{(3)}_n\right]$$
$$\left(\text{for } l = \left[\frac{n}{2}\right]+1 \text{ with even } n\right). \tag{A.4}$$

Fig.2(e) + Fig.2(f) gives

$$\begin{aligned}
&\frac{g^2}{16\pi^2\varepsilon}\left[\sum_{m=2}^{l-1}\left\{(2C_F - C_G)\left(\frac{(-1)^{l-m}\,{}_{l-2}C_{l-m}}{(l-m)\,{}_{n-m+1}C_{l-m}} + \frac{(-1)^{n-l-m}\,{}_{n-l}C_{m-2}}{(n-l+2-m)\,{}_{n-m+1}C_{l-1}}\right)\right.\right.\\
&\quad\left.- C_G\left(\frac{1}{l}+\frac{1}{n-l+2}\right)\right\}\mathcal{R}^{(3)}_{n,m}\\
&\quad+\left\{(2C_F - C_G)\frac{(-1)^n(l-1)}{(n-2l+2)(n-l+1)} - 2C_F(S_{l-1}+S_{n-l+1}-2)\right.\\
&\quad\left.-C_G\left(\frac{1}{l}+\frac{2}{n-l+2}\right)\right\}\mathcal{R}^{(3)}_{n,l}\\
&\quad+\left\{\sum_{m=l+1}^{\langle n/2\rangle}(2C_F - C_G)\left(\frac{(-1)^{m-l}\,{}_{n-l}C_{m-l}}{(m-l)\,{}_{m-1}C_{m-l}} + \frac{(-1)^{n-l-m}\,{}_{n-l}C_{m-2}}{(n-l+2-m)_{n-m+1}C_{l-1}}\right)\right.\\
&\quad\left.- C_G\frac{2}{n-l+2}\right\}\mathcal{R}^{(3)}_{n,m}\\
&\quad\left\{+\left\{(2C_F - C_G)\left(\frac{(-1)^{\frac{n}{2}-l+1}}{\frac{n}{2}-l+1}\frac{{}_{n-l}C_{\frac{n}{2}-l+1}}{{}_{\frac{n}{2}}C_{\frac{n}{2}-l+1}}\right) - C_G\frac{1}{n-l+2}\right\}\mathcal{R}^{(3)}_{n,\frac{n}{2}+1}\quad n:\ \text{even}\right\}\\
&\quad- C_G\left(\frac{1}{l}+\frac{1}{n-l+2}\right)\mathcal{E}^{(3)}_n\Big]\qquad\left(2\le l\le\left\langle\frac{n}{2}\right\rangle\right),
\end{aligned}\tag{A.5}$$

and

$$\begin{aligned}
&\frac{g^2}{16\pi^2\varepsilon}\left[\sum_{m=2}^{n/2}\left\{(2C_F - C_G)\frac{2(-1)^{\frac{n}{2}+1-m}\,{}_{\frac{n}{2}-1}C_{m-2}}{(\frac{n}{2}+1-m)\,{}_{n-m+1}C_{\frac{n}{2}}} - C_G\frac{2}{\frac{n}{2}+1}\right\}\mathcal{R}^{(3)}_{n,m}\right.\\
&\qquad\left.+\left\{4C_F(1-S_{\frac{n}{2}}) - C_G\frac{2}{\frac{n}{2}+1}\right\}\mathcal{R}^{(3)}_{n\frac{n}{2}+1} - C_G\frac{2}{\frac{n}{2}+1}\mathcal{E}^{(3)}_n\right]\\
&\qquad\left(\text{for } l=\frac{n}{2}+1 \text{ with even } n\right).
\end{aligned}\tag{A.6}$$

Fig.2(g) + Fig.2(h) gives

$$\begin{aligned}
&\frac{g^2}{16\pi^2\varepsilon}C_G\left[\sum_{m=2}^{l-1}\frac{1}{2}\left(\frac{(l-3)(l+1-m)}{[l-1]_3}+\frac{l+2}{[l-1]_2}\right.\right.\\
&\quad\left.+\frac{(n-l-1)(n-l+3-m)}{[n-l+1]_3}+\frac{n-l+4}{[n-l+1]_2}\right)\mathcal{R}^{(3)}_{n,m}\\
&\quad+\frac{1}{2}\left(\frac{l-3}{[l-1]_3}+\frac{l+2}{[l-1]_2}+\frac{(n-l-1)(n-2l+4)}{[n-l+1]_3}+2\frac{n-l+4}{[n-l+1]_2}\right)\mathcal{R}^{(3)}_{n,l}
\end{aligned}$$

$$+\sum_{m=l+1}^{\langle n/2\rangle}\frac{1}{2}\left(\frac{(n-l-1)(n-2l+4)}{[n-l+1]_3}+\frac{2(n-l+4)}{[n-l+1]_2}\right)\mathcal{R}^{(3)}_{n,m}$$
$$\left\{+\frac{1}{2}\left(\frac{(n-l-1)(\frac{n}{2}-l+2)}{[n-l+1]_3}+\frac{n-l+4}{[n-l+1]_2}\right)\mathcal{R}^{(3)}_{n,\frac{n}{2}+1}\quad n:\ \text{even}\right\}$$
$$+\left(\frac{1}{l+1}+\frac{1}{n-l+3}\right)\mathcal{E}^{(3)}_n\Big]\qquad\left(2\le l\le\left\langle\frac{n}{2}\right\rangle\right),\tag{A.7}$$

and

$$\frac{g^2}{16\pi^2\varepsilon}C_G\left[\sum_{m=2}^{\frac{n}{2}+1}\left(\frac{\left(\frac{n}{2}-2\right)\left(\frac{n}{2}+2-m\right)}{[\frac{n}{2}]_3}+\frac{\frac{n}{2}+3}{[\frac{n}{2}]_2}\right)\mathcal{R}^{(3)}_{n,m}+\frac{2}{\frac{n}{2}+2}\mathcal{E}^{(3)}_n\right]$$
$$\left(\text{for } l=\frac{n}{2}+1 \text{ with even } n\right).\tag{A.8}$$

Next we calculate Z_{lE}, Z_{lN}, Z_{EE} and Z_{NN} from the one-loop two-point functions shown in Fig. 3 with a nonzero quark mass.

The one-loop correction to the two-point function with $R_{n,l}\cdot\Delta$ comes from Fig. 3 (b) and (c). It gives

$$\frac{g^2}{16\pi^2\varepsilon}C_F\left[-\left(\frac{2}{[l]_2}+\frac{2}{[n-l+2]_2}\right)\mathcal{E}^{(2)}_n\right.$$
$$\left.+\left(\frac{4}{[l-1]_3}+\frac{4}{[n-l+1]_3}\right)\mathcal{N}^{(2)}_n\right].\tag{A.9}$$

For the one-loop correction to the two-point function with $E_n\cdot\Delta$, Fig.3(a) gives

$$\frac{g^2}{16\pi^2\varepsilon}C_F\left[\frac{4}{n+1}\mathcal{E}^{(2)}_n+2\frac{n-1}{[n]_2}\mathcal{N}^{(2)}_n\right]\tag{A.10}$$

and Fig.3(b)+Fig.3(c) gives

$$\frac{g^2}{16\pi^2\varepsilon}C_F\left[\left(3-\frac{4}{n+1}-2S_n\right)\mathcal{E}^{(2)}_n-\left(3+\frac{2(n-1)}{[n]_2}\right)\mathcal{N}^{(2)}_n\right].\tag{A.11}$$

Although each contribution from Fig. 3 (a) and (b) is different from the one for h_L, the sum of (A.10) and (A.11) are the same as the one for h_L.

Finally, for the one-loop correction to the two-point function with $N_n\cdot\Delta$, Fig.3(a) gives

$$\frac{g^2}{16\pi^2\varepsilon}C_F\frac{2}{n(n+1)}\mathcal{N}^{(2)}_n,\tag{A.12}$$

and each of Figs.3 (b) and (c) gives the same contribution,

$$\frac{g^2}{16\pi^2\varepsilon}C_F\left(-2\sum_{j=2}^{n}\frac{1}{j}\right)\mathcal{N}^{(2)}_n.\tag{A.13}$$

These are the same as the ones for h_L.

References

[1] K. Abe et al., Phys. Rev. Lett. **76**, 587 (1996).

[2] R.L. Jaffe and X. Ji, Phys. Rev. Lett. **67**, 552 (1991); Nucl. Phys. **B375**, 527 (1992).

[3] E.V. Shuryak and A.I. Vainshtein, Nucl. Phys. **B201**, 141 (1982);
A.P. Bukhvostov, E.A. Kuraev and L.N. Lipatov, Sov. Phys. JETP **60**, 22 (1984);
P.G. Ratcliffe, Nucl. Phys. **B264**, 493 (1986);
I.I. Balitsky and V.M. Braun, Nucl. Phys. **B311**, 541 (1988/89);
X. Ji and C. Chou, Phys. Rev **D42**, 3637 (1990);
J. Kodaira, K. Tanaka, T. Uematsu and Y. Yasui, hep-ph 9603377.

[4] A. Ali, V.M. Braun and G. Hiller, Phys. Lett. **B266**, 117 (1991).

[5] J. Kodaira, Y. Yasui and T. Uematsu, Phys. Lett. **B344**, 348 (1995).

[6] Y. Koike and K. Tanaka, Phys. Rev. **D51**, 6125 (1995).

[7] I.I. Balitsky, V.M. Braun, Y. Koike and K. Tanaka, hep-ph/9605439, Phys. Rev. Lett. in press.

[8] R.L. Jaffe and X. Ji, Phys. Rev. Lett. **71**, 2457 (1993);
X. Ji, Phys. Rev. **D49**, 114 (1994).

[9] V.N. Gribov and L.N. Lipatov, Sov. J. Nucl. Phys. **15**, 675 (1972).

[10] V.N. Gribov and L.N. Lipatov, Sov. J. Nucl. Phys. **15**, 438 (1972);
L.N. Lipatov, *ibd.* **20**, 94 (1975);
G. Altarelli and G. Parisi, Nucl. Phys. **B126**, 298 (1977).

Figure captions

Fig. 1. (a) Three-point basic vertex for $R_{n,l}$, E, and N. (b) Four-point basic vertex for $R_{n,l}$ necessary for the calculation of the diagrams shown in Fig. 2.

Fig. 2. One-particle-irreducible diagrams for the one-loop correction to $F_\mu(p,q,k)$.

Fig. 3. One-loop corrections to the two-point functions.

Fig. 4. (a) Complete spectrum of the exact eigenvalues of the anomalous dimension matrix for $e(x,Q^2)$ together with those for h_1 (squares). (b) Complete spectrum of the leading N_c eigenvalues of the anomalous dimension matrix for $e(x,Q^2)$. Solid line is the analytic solution in (4.1).

(a) (b)

Fig.1

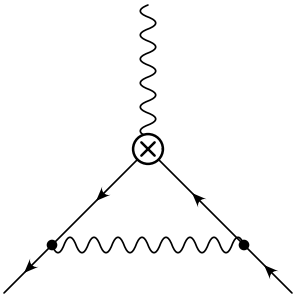

(a)

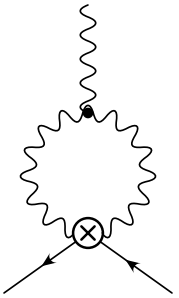

(b)

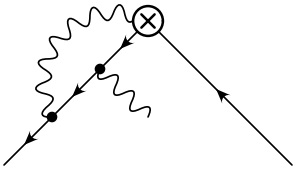

(c)

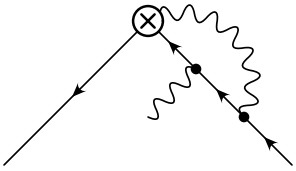

(d)

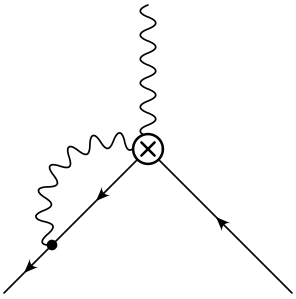

(e)

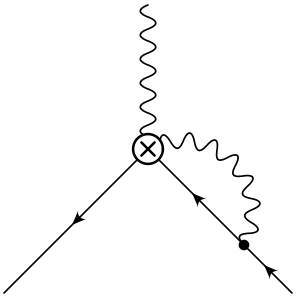

(f)

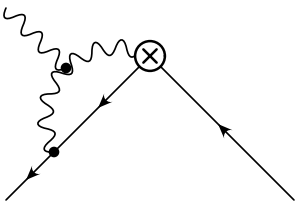

(g)

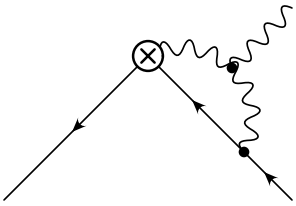

(h)

Fig.2

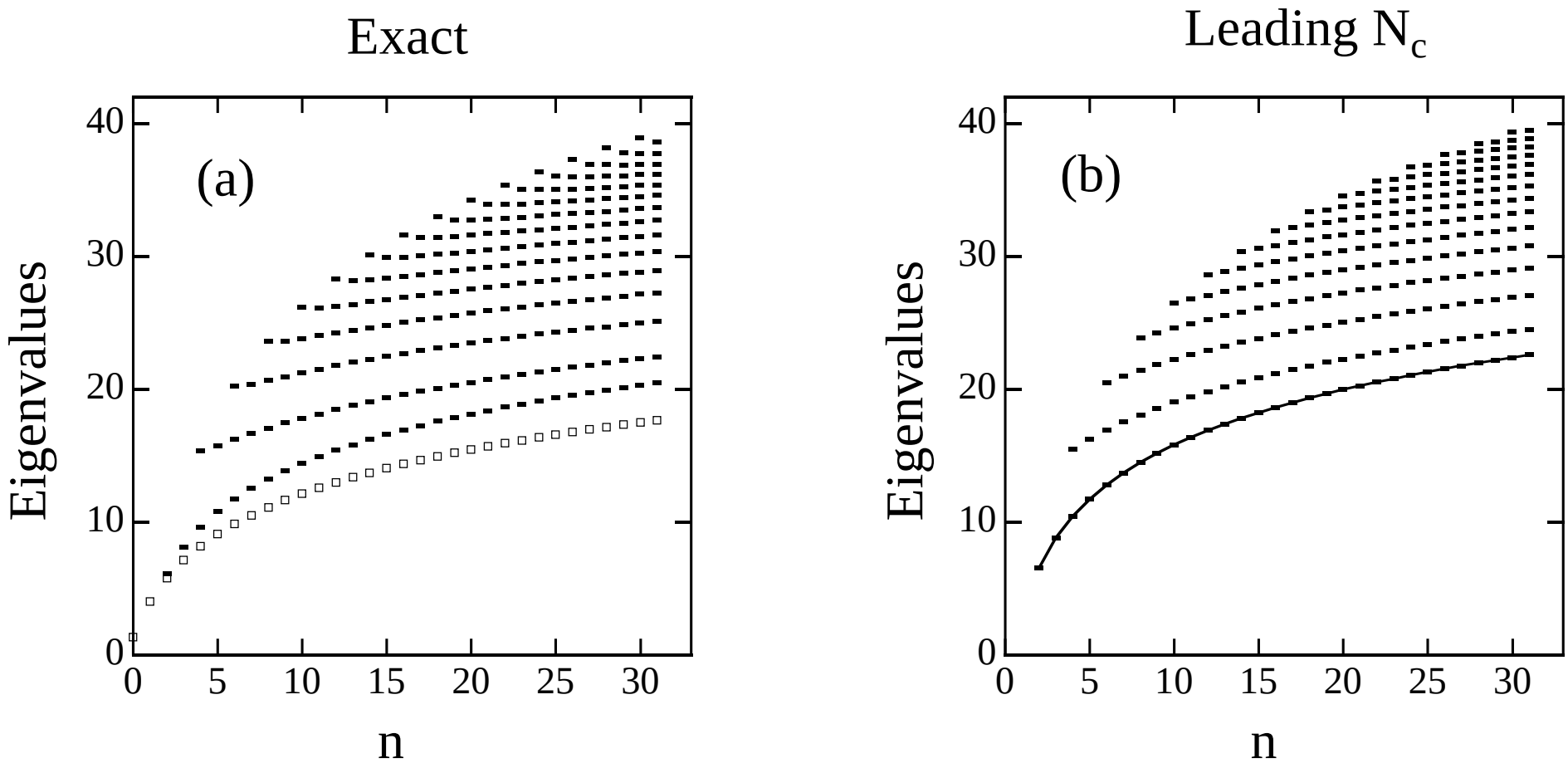
Exact
Leading N_c
(a)
(b)
Eigenvalues
Eigenvalues
n
n
0
10
20
30
40
0
5
10
15
20
25
30

Fig.4

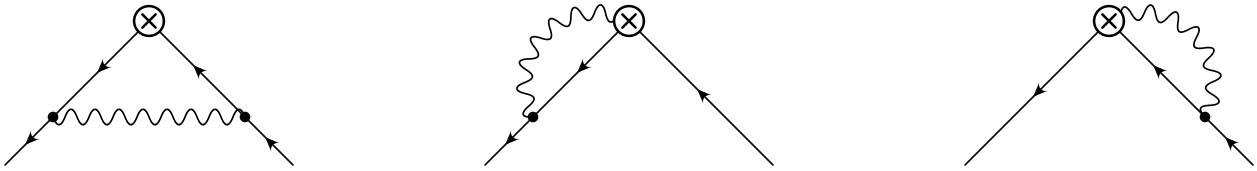

(a) (b) (c)

Fig.3